Ag(I)-Catalyzed Chlorination of Linezolid during Water Treatment: Kinetics and Mechanism

RAVIRAJ M. KULKARNI,[1] MANJUNATH S. HANAGADAKAR,[2] RAMESH S. MALLADI,[1] NAGARAJ P. SHETTI[3]

[1]*Department of Chemistry, KLS Gogte Institute of Technology (Autonomous), Affiliated to Visvesvaraya Technological University, Belagavi, 590 008, India*

[2]*Department of Chemistry, SJPN Trust's Hirasugar Institute of Technology, Affiliated to Visvesvaraya Technological University, Nidasoshi, 591 236, India*

[3]*Department of Chemistry, KLE Institute of Technology, Affiliated to Visvesvaraya Technological University, Hubballi, 580 030, India*

Received 4 August 2017; revised 19 January 2018; accepted 11 March 2018

DOI 10.1002/kin.21175
Published online 26 April 2018 in Wiley Online Library (wileyonlinelibrary.com).

ABSTRACT: The kinetic and mechanistic study of Ag(I)-catalyzed chlorination of linezolid (LNZ) by free available chlorine (FAC) was investigated at environmentally relevant pH 4.0–9.0. Apparent second-order rate constants decreased with an increase in pH of the reaction mixture. The apparent second-order rate constant for uncatalyzed reaction, e.g., $k''_{app} = 8.15$ dm^3 mol^{-1} s^{-1} at pH 4.0 and $k''_{app.} = 0.076$ dm^3 mol^{-1} s^{-1} at pH 9.0 and 25 ± 0.2°C and for Ag(I) catalyzed reaction total apparent second-order rate constant, e.g., $k''_{app} = 51.50$ dm^3 mol^{-1} s^{-1} at pH 4.0 and $k''_{app.} = 1.03$ dm^3 mol^{-1} s^{-1} at pH 9.0 and 25 ± 0.2°C. The Ag(I) catalyst accelerates the reaction of LNZ with FAC by 10-fold. A mechanism involving electrophilic halogenation has been proposed based on the kinetic data and LC/ESI/MS spectra. The influence of temperature on the rate of reaction was studied; the rate constants were found to increase with an increase in temperature. The thermodynamic activation parameters E_a, $\Delta H^{\#}$, $\Delta S^{\#}$, and $\Delta G^{\#}$ were evaluated for the reaction and discussed. The influence of catalyst, initially added product, dielectric constant, and ionic strength on the rate of reaction was also investigated. The monochlorinated substituted product along with degraded one was formed by the reaction of LNZ with FAC.
 Int J Chem Kinet 50: 495–506, 2018

Correspondence to: R. M. Kulkarni; e-mail: ravirajmk@git.edu.
Supporting Information is available in the online issue at www.wileyonlinelibrary.com.

INTRODUCTION

Chemical oxidizing agents, such as chlorine, chlorine dioxide, chloramines, and ozone, have ability to

disinfect microorganisms. Hence, they are commonly used in water treatment processes. They are also used for taste and odor control and to oxidize microcontaminants. But, in certain circumstances, oxidizing agents having ability to form toxic by-products or they may react with micropollutants present in water bodies. High oxidation potential and low cost makes chlorine an efficient disinfectant in municipal water treatment plants. Chlorination is mainly carried out to remove ammonia and to maintain residual chlorine in the water distribution system [1,2]. Hypochlorous acid (HOCl) and hypochlorite (OCl^-) are the main chlorine species, which are called free available chlorine (FAC). HOCl and OCl are predominant species at pH below 7.5 and above 7.5, respectively [3].

Chemical removal methods generate by-products, which eventually enter the environment as aquatic toxic pollutants. Physicochemical methods used for treatment of pollutants in wastewater are adsorption, electrolytic oxidation, and H_2O_2 [4,5]. During the oxidation process, oxidizing agents transform these toxic substances to less harmful compounds that are safe to be discharged to the environment [6].

In recent years, research has confirmed the presence of several antibacterial agents in the water environment [7–9]. The presence of antibiotics in the environment has led to numerous studies, investigating the role of specific environmental and water treatment methods. Environmental processes related to adsorption and/or oxidation within soils and sediments [10–12], photolysis, and biodegradation have all been previously investigated in depth [13–15]. Linezolid (LNZ) has a 1,3-oxazolidinone moiety containing an acetamide subgroup at the fifth methyl group position. LNZ has been widely used as a human and veterinary drug for the treatment of diseases and as a food supplement to improve body mass of farm animals [16]. LNZ belongs to the oxazolidinone class of antimicrobial agents and is nonbiodegradable. The pharmaceuticals of this antibacterial group have been identified as emerging environmental contaminants. The principal route for the entry of antibacterial agents in the aquatic environment is through the incomplete metabolism of these compounds within the human body; a large fraction of the clinically prescribed oxazolidinone class of antimicrobial agents is discharged into municipal wastewater systems [17].

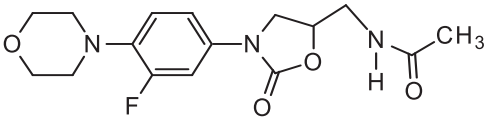

Silver is one of the commonly used transition metals (d block element) as a catalyst in the industry. The Ag(I) ions are also used to catalyze the intermolecular molecular carbene insertion in C–X bonds (X = halogen), C–H, and aromatic systems [18–20]. The direct oxidation of alcohols, oxidative activation of alkenes, and also simple alkanes has received considerable attention [21]. The silver ions were used in the synthesis of organic and inorganic compounds as a Lewis acid catalyst [22]. Silver is used as a disinfectant in washing machines to clean clothes. So, a trace amount of silver may enter the water system [23].

There are no reports on the Ag(I)-catalyzed kinetic investigation of LNZ by any oxidants. Hence, the reaction of LNZ with FAC with and without the Ag(I) catalyst was carried out to understand the mechanism and identify the role of Ag(I) as a catalyst in water treatment processes.

EXPERIMENTAL

Materials and Reagents

All the chemicals were used in this research are of analytical grade and prepared in deionized water. A stock solution of LNZ (99.8% purity; a gift from Dr. Reddy's Laboratories, Hyderabad, India.) was prepared by dissolving adequate amount of sample in deionized water. The purity of the LNZ was further confirmed by the single peak at 338.18 m/z ($M + H^+$) in ESI LCMS. The FAC solution was prepared by taking appropriate volume of 5% NaOCl (Thomas Baker) in distilled water according to the procedure explained elsewhere [24]. A stock solution of silver nitrate ($AgNO_3$) (Himedia, Mumbai, India) of known concentration was prepared in chlorine-free distilled water. The iodometry and DPD-FAS titrimetry method were used for the standardization of stock solution of FAC. A stock solution of chlorine was prepared by using 5% NaOCl (Thomas Baker) in a distilled water aliquot diluted to 100 mL. Five milliliters of 0.1 N KI solution was added to 2 mL of phosphate buffer and 2 mL of DPD (diethyl-*p*-phenylene diamine) indicator and titrated with the standard FAS (ferrous ammonium sulfate) solution until the red color was obtained. The volume of FAS used in the titration was used to calculate amount of chlorine (in mg/L) [25,26]. Buffer solutions of 0.02 M acetate (pH 4.0–5.0), phosphate (pH 6.4–7.0), and borate (pH 8.0–9.0) were used to keep the pH constant throughout the experiment. To study the effect of initially added products, chloramines were prepared by the reaction of ammonia with sodium hypochlorite [27].

Instruments Used

i. A UV–vis spectrophotometer (Cary 50 Bio, Varian BV) and a HPLC system (Shimadzu Prominence) were used for kinetic measurements.
ii. A Thermo Scientific Q Exactive high-resolution mass spectrophotometer (HR-MS) was used; a Thermo Scientific Hypersil Gold C18 (150 × 4.6 mm-8 μm) column was used for product analysis.
iii. pH measurements were done with a pH meter (Elico LI 120).

Kinetic Measurements

The kinetic investigations were carried out by keeping [FAC] ≫ [LNZ] to maintain pseudo–first-order conditions, and the buffers with 0.02 M were used to maintain the ionic strength. The reaction was initiated by mixing FAC, silver nitrate ($AgNO_3$), and LNZ with a required volume of buffers in the thermostat at 25 ± 0.2°C. The progress of the reaction was studied conveniently by measuring the absorbance of LNZ at 252 nm, which decreases with time. The UV–vis spectral changes in the presence of Ag(I) during the chlorination of LNZ by the FAC catalyst are shown in Fig. 1.

The application of Beer's law of LNZ at λ_{max} 252 nm was verified, yielding $\varepsilon = 32{,}620\ dm^3\ mol^{-1}\ cm^{-1}$ and the first-order constants (k_{obs}) were evaluated from the plots of log $(A_t - A_\infty)$ versus time by fitting the data to the expression $A_t = A_\infty + (A_0 - A_\infty)\ e^{-kt}$, where A_t, A_0, and A_∞ are absorbances of LNZ at time t, 0 and ∞, respectively. The plots were linear up to about 60% completion of the reaction, and the rate constants were reproducible within ±8%. $A_t - A_\infty$ was taken to avoid the possible interference from the products [28]. The parent compound loss was also monitored by the HPLC system (Agilent 1100 series) with a RX-C18 column (4.6 mm × 250 mm, 5 μm) with a UV diode array detector. The observed rate constants obtained from the HPLC method were in good agreement with UV–vis methods with an experimental error of ±8%. The FAC concentration was measured by DPD-FAS titrimetry [26] at the conclusion of each kinetic experiment. The completion of the reaction was checked by LC/ESI/MS.

Product Identification Method

LNZ was added to 10 mM phosphate buffer (pH 7) to attain a starting concentration of 100 mg dm^{-3}. The FAC solution was accordingly added to start the reactions at oxidant: substrate molar ratios varying from 1:2 to 5:1. This mixture was allowed to react via the oxidation kinetics of LNZ by chlorine in a neutral medium for the period of 12 h in a closed container at 25 ± 0.2°C. After completion of reaction, a small amount of the reaction mixture was taken and filtered before injecting into HPLC and HR-MS systems in which a Thermo Scientific Hypersil Gold C18 column (150 × 4.6 mm × 8 μm) was fitted for the separation and identification of degraded components of the reaction mixture. To carry the reaction mixture, the mobile phase (acetonitrile: water ratio 50:50) was used with the flow rate of 500 μL/min and pressure (33.2 bar) throughout the analysis of components of the reaction mixture. The soft technique ESI^+ (positive mode electro spray ionization) was used for the product identification. With the help of the HR-MS system, the chromatogram and mass spectrum of the reaction mixture were recorded over the mass scan range of 250–420 m/z. The HPLC and mass spectra of standard LNZ and its product are shown in Fig. S1 (in the Supporting Information). Pure LNZ shows a single peak at retention time (t_R) 4.10 min, and its mass is 338.15. The LNZ/FAC reaction shows a single peak at retention time (t_R) 3.87 min, and its protonated peak [M + H^+] 372.15 indicates completion of the reaction and also infers that one fundamental reaction product is formed. The major and

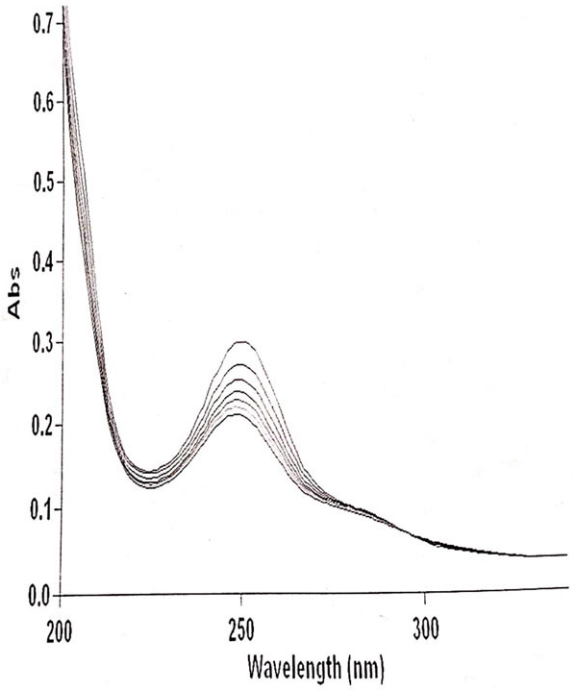

Figure 1 UV–vis spectral changes during the chlorination of LNZ in the presence of the Ag(I) catalyst by FAC at 25 ± 0.2°C. [Color figure can be viewed at wileyonlinelibrary.com]

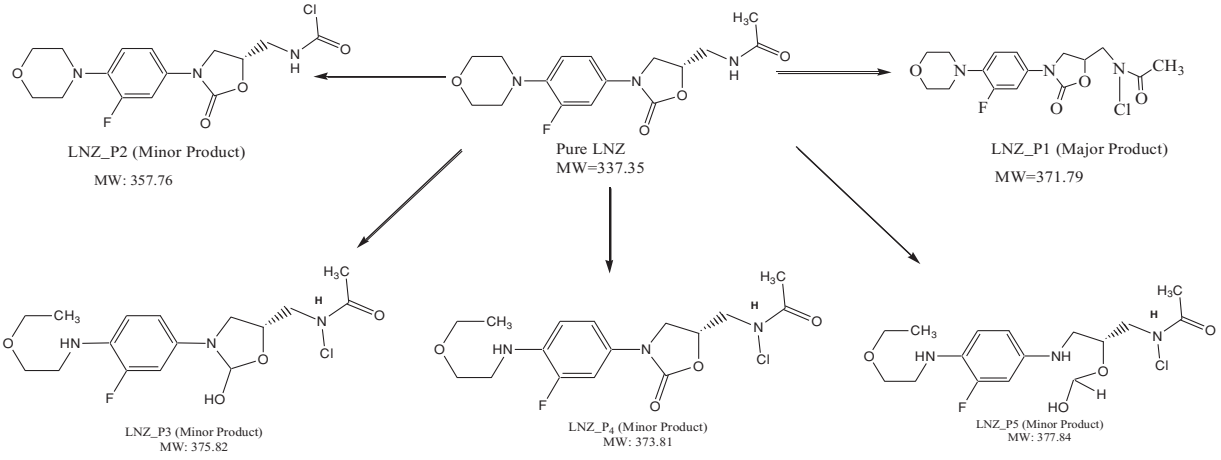

Scheme 1 Chlorinated and degraded products of LNZ.

minor identified LC-ESI-MS products in the reaction are presented in Scheme 1 and Table I. The proposed mechanism for the major LNZ product of uncatalyzed and catalyzed reactions is shown in Schemes 2 and 3.

The proposed mechanism involves the formation of a complex that reacts with the substrate at rate-determining steps to form a complex followed by a slow reaction giving rise to a chlorinated product [16].

RESULTS AND DISCUSSION

Kinetic Modeling

The reaction of LNZ with FAC is first order with respect to each reactant and hence can be treated as second order and described with a second-order rate equation:

$$\frac{\mathrm{d[LNZ]_T}}{\mathrm{d}t} = k'_{\mathrm{obs}}[\mathrm{LNZ}]_\mathrm{T} = k''_{\mathrm{app}}[\mathrm{FAC}]_\mathrm{T}[\mathrm{LNZ}]_\mathrm{T} \quad (1)$$

where k'_{obs} is the pseudo–first-order rate constant, T for a given reactant denotes the sum of all acid-base species, and k''_{app} represents the pH-dependent apparent second-order rate constant for the overall reaction, which can be calculated from $k''_{\mathrm{app}} = (k'_{\mathrm{obs}}/[\mathrm{FAC}]_\mathrm{T})$. The variation in k''_{app} from pH 4.00 to 9.00 can be ascribed to the varying importance of the specific reaction among the individual acid-base speciation of LNZ and FAC. The acid-base speciation of FAC and LNZ can be modeled by

$$\mathrm{HOCl} \overset{K_a,\mathrm{HOCl}}{\rightleftharpoons} \mathrm{OCl^-} + \mathrm{H^+}$$

The decrease in the value of k''_{app} above pH 7.50 can be ascribed to deprotonation of HOCl to yield $\mathrm{OCl^-}$, which is generally a much weaker electrophile than HOCl [16].

Table I Chlorination and Degraded Products of LNZ

Linezolid Chlorination Products	Measured Molecular Ion Peak ($M + H^+$)	Theoretical Mass of Products (Da)	Molecular Formulae of the Products	Measured Mass – Theoretical Mass
Linezolid_P1	371.11	371.79 (Major product)	$C_{16}H_{19}ClFN_3O_4$	−0.68
Linezolid_P2	357.16	357.76 (Minor Product)	$C_{15}H_{17}ClFN_3O_4$	−0.60
Linezolid_P3	375.11	375.82 (Minor Product)	$C_{16}H_{23}ClFN_3O_4$	−0.71
Linezolid_P4	374.11	373.81 (Minor Product)	$C_{16}H_{21}ClFN_3O_4$	+0.30
Linezolid_P5	378.92	377.84 (Minor Product)	$C_{16}H_{25}ClFN_3O_4$	+1.08

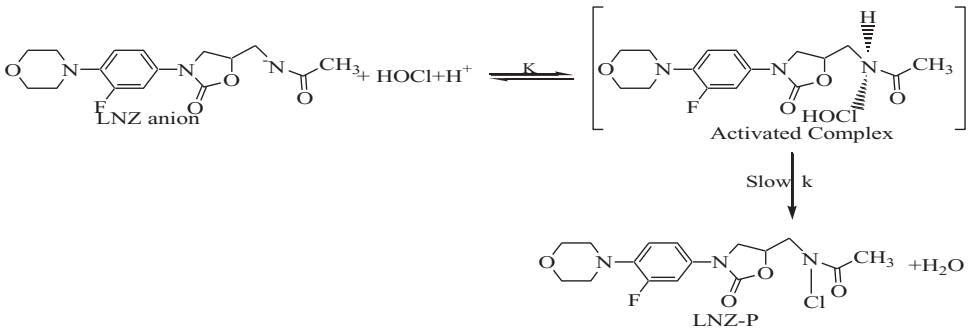

Scheme 2 Proposed mechanism for uncatalyzed LNZ/FAC reaction based on kinetic data and LC-MS spectra.

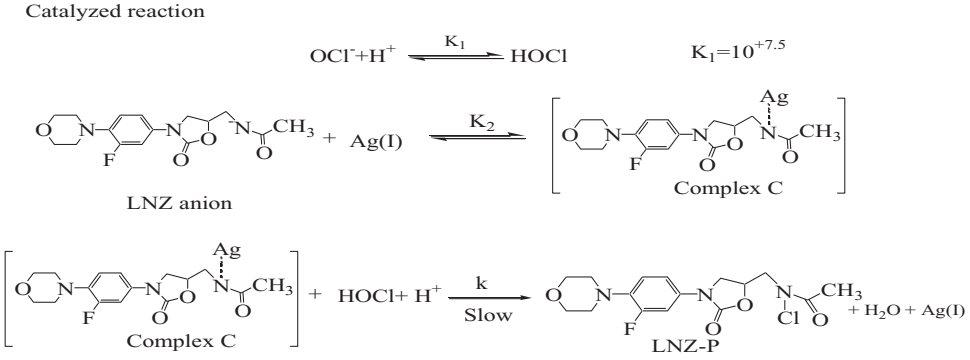

Scheme 3 Complete reaction scheme for Ag(I) catalyzed oxidation of LNZ by FAC.

Reaction Order

The oxidation of LNZ with FAC takes place with a measurable rate in the reaction without the use of Ag(I), and the catalytic reaction is believed to take place in an almost identical way in both uncatalyzed and catalyzed reactions. Therefore, the total rate constant (k_T) is equal to the addition of the rate constants of the uncatalyzed (k_U) and catalyzed (k_C) reactions: $k_C = k_T - k_U$.

Thus the experimental reaction orders are calculated from the slopes of log k'_{obs} vs. log [Concentration] plots by changing the concentrations of LNZ, FAC, and catalyst Ag(I), while rest of conditions remained constant.

The uncatalyzed reaction was studied by changing the concentrations of LNZ and FAC, while retaining the others conditions constant. For the uncatalyzed reaction (k_U), rate constants were determined by the plot of log k'_{obs} vs. time.

Influence of [LNZ]

The concentration of LNZ was changed from 0.50×10^{-5} to 2.50×10^{-5} M, while other reactant concentrations and reaction conditions were kept constant. The plots of log [absorbance] vs. time, used for different initial concentrations of LNZ in both catalyzed and uncatalyzed reactions, are found to be linear, showing that the order with respect to [LNZ] was unity [16]. The pseudo–first-order rate constant remains the same as shown in Table I.

Influence of [FAC]

The FAC concentration was varied from 0.50×10^{-4} M to 2.50×10^{-4} M at constant concentrations of LNZ: 1.00×10^{-5} M, Ag(I); 1.00×10^{-8} M and at constant ionic strength of 0.01 M at pH 4.00, 5.00, 6.40, 7.00, 8.00, and 9.00 as shown in Table I. The plot of log k'_{obs} vs. log [FAC] was linear with slope equaling unity, indicating first order with respect to FAC. It is observed that the pseudo–first-order rate constants k'_{obs} increase with an increase in the concentration of FAC.

Influence of pH

The pH of the reaction mixture was varied from pH 4.00 to 9.00 using acetate, phosphate, and borate buffers, while maintaining the other reaction conditions constant during the experiment. The rate constants are observed to decrease with an increase in pH (Table II).

Table II Influence of Variation of [FAC], on the Silver-Catalyzed Chlorination of LNZ at 25°C. I = 0.01M at Different pH Values

pH	10^4 [FAC] (M)	10^5 [LNZ] (M)	10^8 [Ag^+] (M)	$10^4\ k'_{obs\ T.}$ (s^{-1}) (Total) Found	$10^5\ k'_{obs\ U}$ (s^{-1}) (Uncatalyzed)	$10^4\ k'_{obs\ C}$ (s^{-1}) (Catalyzed)
4.00	0.50	1.00	1.00	3.06	7.40	2.32
	1.00	1.00	1.00	6.13	17.00	4.43
	1.50	1.00	1.00	18.30	57.50	12.55
	2.00	1.00	1.00	43.20	99.00	33.30
	2.50	1.00	1.00	69.80	139.00	55.90
5.00	0.50	1.00	1.00	1.81	4.35	1.37
	1.00	1.00	1.00	4.30	19.70	2.33
	1.50	1.00	1.00	12.83	30.90	9.74
	2.00	1.00	1.00	18.60	52.10	13.39
	2.50	1.00	1.00	30.80	60.20	24.78
6.40	0.50	1.00	1.00	1.11	3.22	0.79
	1.00	1.00	1.00	4.27	12.10	3.06
	1.50	1.00	1.00	10.80	19.70	8.83
	2.00	1.00	1.00	15.00	26.10	12.39
	2.50	1.00	1.00	21.10	31.80	17.92
7.00	0.50	1.00	1.00	0.86	3.53	0.51
	1.00	1.00	1.00	1.20	5.56	0.64
	1.50	1.00	1.00	2.27	8.32	1.44
	2.00	1.00	1.00	3.18	12.20	1.96
	2.50	1.00	1.00	4.33	13.50	2.98
7.00	1.50	0.50	1.00	2.19	8.56	1.33
	1.50	1.00	1.00	2.12	8.32	1.28
	1.50	1.50	1.00	2.27	8.38	1.44
	1.50	2.00	1.00	2.56	8.52	1.71
	1.50	2.50	1.00	2.81	8.73	1.93
8.00	0.50	1.00	1.00	0.47	1.69	0.30
	1.00	1.00	1.00	0.93	2.61	0.67
	1.50	1.00	1.00	1.20	4.72	0.73
	2.00	1.00	1.00	2.54	5.18	2.02
	2.50	1.00	1.00	3.01	5.25	2.49
9.00	0.50	1.00	1.00	0.38	0.56	0.32
	1.00	1.00	1.00	0.62	1.08	0.51
	1.50	1.00	1.00	0.97	1.68	0.80
	2.00	1.00	1.00	1.35	1.63	1.19
	2.50	1.00	1.00	2.60	2.19	2.38
7.00	1.50	0.50	1.00	2.19	8.56	1.33
	1.50	1.00	1.00	2.12	8.32	1.28
	1.50	1.50	1.00	2.27	8.38	1.44
	1.50	2.00	1.00	2.56	8.52	1.71
	1.50	2.50	1.00	2.81	8.73	1.93
7.00	1.00	1.00	1.00	1.20	–	1.20
	1.00	1.00	2.00	7.34	–	7.34
	1.00	1.00	3.00	8.77	–	8.77
	1.00	1.00	4.00	16.70	–	16.70
	1.00	1.00	5.00	25.20	–	25.20
	1.00	1.00	6.00	30.50	–	30.50
	1.00	1.00	7.00	39.00	–	39.00

Error ± 8%.

The second-order rate constants are also evaluated with the plot of k'_{obs} vs. [FAC] for corresponding pH values (Fig. 2). A graph of k''_{app} vs. pH (Fig. 3) shows the pH dependence of the apparent second-order rate constants for the total Ag(I)-catalyzed chlorine reaction with LNZ.

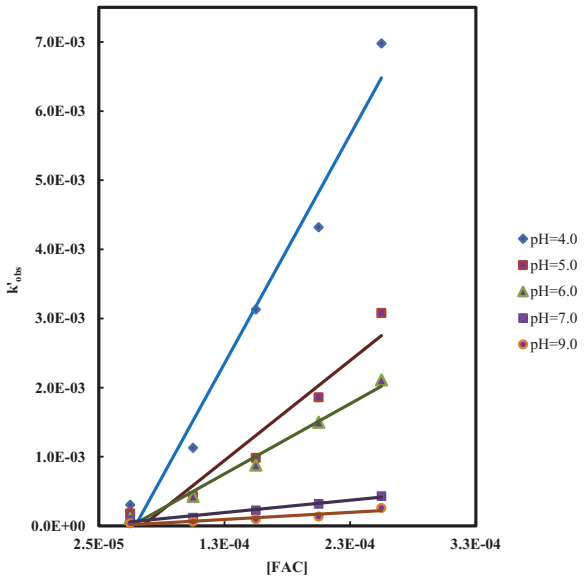

Figure 2 Second-order plot of k'_{obs} vs. [FAC]. [Color figure can be viewed at wileyonlinelibrary.com]

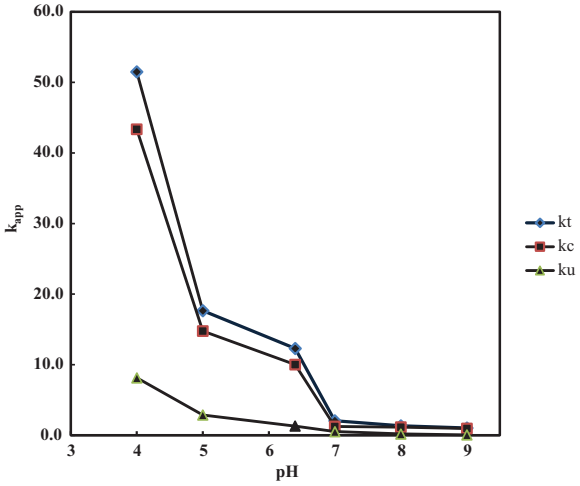

Figure 3 Second-order rate constants; catalyzed, uncatalyzed, and total reaction plot of k''_{app} vs. pH. [Color figure can be viewed at wileyonlinelibrary.com]

The pH-dependent apparent second-order rate constant for the catalyzed and uncatalyzed reactions was calculated from the plot of $k''_{app} = (k'_{obs.}/[FAC]_T)$. The variation in $k''_{app.}$ from pH 4.00 to 9.00 can be attributed to the varying importance of specific reaction among the individual acid–base conditions of LNZ and FAC. LNZ has a pK_a value of 1.8, which indicates that it exists as an anion in aqueous media with pH > 4 [29]. The variation in k''_{app} from pH 4.00 to 9.00 can be ascribed to the changing importance of specific reactions among the individual acid–base speciation of FAC. The decrease in the value of k''_{app} above pH 7.0 can be ascribed to deprotonation of HOCl to yield OCl^-, which is generally a much weaker electrophile than HOCl [16].

Influence of Ionic Strength

The effect of ionic strength (I) at 25°C was determined by changing the buffer concentration from 8.0×10^{-4} M to 8.0×10^{-3} M at pH 5.00, 7.00, and 9.00. The rate constants were found to remain almost constant. It was observed that the ionic strength had an insignificant effect on the rate constant (Table III). The solvent did not react with the oxidant in experimental conditions [30].

Influence of Dielectric Constant

The influence of the dielectric constant (D) was determined by changing the tertiary-butanol water volume in the reaction while other conditions were held constant. The D values were calculated using the equation, $D = D_W V_W + D_B V_B$, where D_B and D_W are dielectric constants of pure tertiary-butanol and water, respectively, and V_W and V_B are the volume portion of components, e.g., water with tertiary butyl alcohol, respectively, in the total volume of the mixture. Determination of the comparative permittivities was unsuccessful, so they were calculated from the data of pure liquids [30]. The rate constant k'_{obs} decreases with a decrease in the dielectric constant of the medium. The graphical plot of log k'_{obs} vs. $1/D$ gives a straight line with a negative slope of -15.67, and $R^2 \geq 0.993$ for the Ag(I)-catalyzed reaction as shown in Fig. 4.

Influence of Initially Added Products

The influence of initially added products was determined by adding common chlorination products, such as chloramines or combined chlorine, to the reaction mixture, and it is observed that the products did not show any considerable influence on the reaction rate.

$$\text{Rate} = -\frac{d[LNZ]}{dt} = kK_1K_2[OCl^-][H^+][LNZ][Ag^+]$$

$$\frac{\text{Rate}}{[LNZ]} = k_{obs} = kK_1K_2[OCl^-]^{1.02}[H^+]^{0.27}[Ag^+]^{1.13}$$

Polymerization Study

For both uncatalyzed and catalyzed reactions, the possible interference of free radicals was examined by adding acrylonitrile to the reaction mixture. It was stored in an inert environment for 24 h. This reaction

Table III Influence of Ionic Strength on the Chlorination of LNZ at Different pH values and at 25 ± 0.2°C, [FAC] = 1.50×10^{-4} M, [LNZ] = 1.00×10^{-5} M, [Ag^+] = 1.00×10^{-8} M, I = 0.01M

pH	10^3 [Buffer] (M)	10^4 $k_{obs.}$ (s^{-1})	pH	10^3 [Buffer] (M)	10^5 $k_{obs.}$ (s^{-1})	pH	10^3 [Buffer] (M)	10^5 $k_{obs.}$ (s^{-1})
	0.80	3.37		0.80	6.14		0.80	1.12
	2.00	3.02		2.00	6.38		2.00	1.05
5.00	4.00	3.06	7.0	4.00	6.69	9.0	4.00	1.49
	6.00	3.67		6.00	6.73		6.00	0.99
	8.00	3.52		8.00	6.99		8.00	1.10

Error ± 8%.

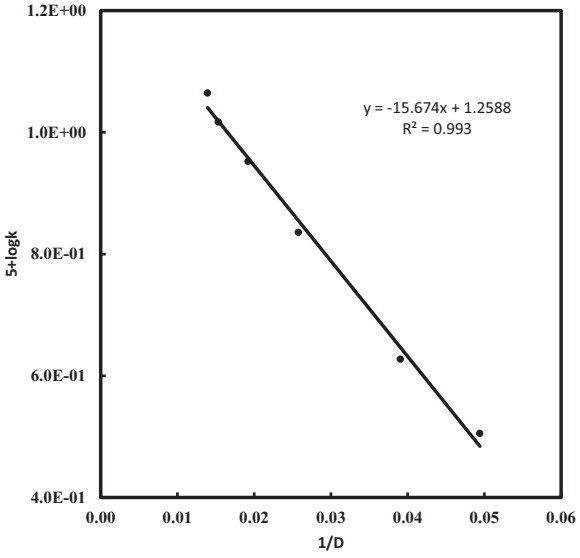

Figure 4 Influence of the dielectric constant on the chlorination of LNZ in the presence of the Ag(I) catalyst.

mixture was diluted by methyl alcohol, and precipitate was not observed, which suggests that free radicals were not involved in the reaction [31,32].

Influence of Temperature

The kinetics of both catalyzed and uncatalyzed reactions at five distinct temperatures was investigated by varying [FAC] concentrations while other experimental conditions remained constant. The rate constant increased with an increase in temperature. The second-order rate constants k''_{app} at five temperatures 15, 20, 25, 35, and 40°C for catalyzed and uncatalyzed reactions are listed in Table IV. The activation energy related to these rate constants was calculated by the Arrhenius plot of log k vs. $1/T$, and other activation parameters as calculated are shown in Table IV. The effort shows the effect of different activation parameters on the reaction mechanism. The activation energies at different pH values were determined as listed in Table IV. The activation energy values were reported for both silver(I)-catalyzed and uncatalyzed reactions in Table IV; it is clear from the table that activation energy increased with the increase in pH. HOCl is the only reactive species at pH values below 5 and OCl^- is the only reactive species above pH 9 [24]. The activation energy at pH 4 is due to the HOCl reaction with LNZ^-, and activation energy at pH 9 is due to the OCl^- reaction with LNZ^-.

Table IV Activation Parameters for the Ag(I)-Catalyzed Oxidation of LNZ by FAC with Respect during the Chlorination Reaction. [LNZ] = 1.00×10^{-5} M, [Ag^+] = 1.00×10^{-8} M, I = 10.0×10^{-3} M, [FAC] = 1.00×10^{-4} M, 1.50×10^{-4} M, 2.00×10^{-4} M, 2.50×10^{-4} M, 3.00×10^{-4} M, and 3.50×10^{-4} M

Effect of Temperature

Temperature (K)	10^3 k_U (s^{-1})	10^3 k_C (s^{-1})
288	2.24	6.53
293	2.54	6.72
298	2.82	7.35
308	3.06	8.01
313	3.19	9.09

Activation Parameters

Activation Parameter	Uncatalyzed	Ag(I) Catalyzed
E_a (kJ mol^{-1})	14.33 ± 1.50	12.07 ± 2.0
$\Delta H^{\#}$ (kJ mol^{-1})	11.85 ± 1.20	9.58 ± 1.0
$\Delta S^{\#}$ (J K^{-1} mol^{-1})	−12.40 ± 1.50	−257.88 ± 1.0
$\Delta G^{\#}$ (kJ mol^{-1})	15.54 ± 1.60	86.95 ± 2.0

Activation Energy at Different pH for LNZ and FAC Reaction

	Activation Energy, E_a (kJ mol^{-1})	
pH	Uncatalyzed	Ag(I) Catalyzed
4.00	13.87 ± 1.50	11.34 ± 2.0
7.00	14.33 ± 1.50	12.07 ± 2.0
9.00	16.99 ± 1.50	13.63 ± 2.0

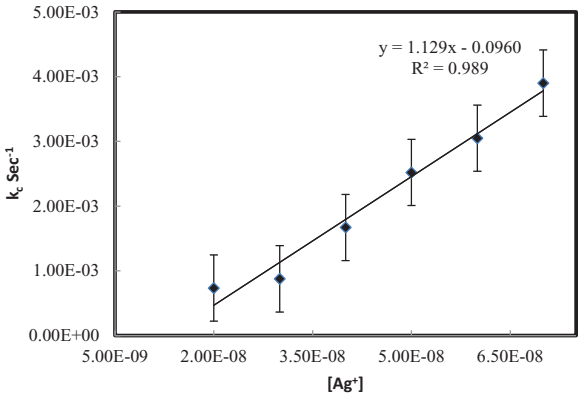

Figure 5 First-order rate constant for the reaction of LNZ and FAC at different concentrations of Ag(I). [Color figure can be viewed at wileyonlinelibrary.com]

Influence of [Ag(I)] Catalyst

The [Ag(I)] catalyst concentrations were changed from 1.00×10^{-8} to 7.00×10^{-8} mol dm^{-3}, at regular concentrations of LNZ, HOCl, and steady ionic strength. The reaction rate increases with an increase in the concentration of Ag(I) (Table I). The order for [Ag(I)] was calculated to be approximately unity from the linearity plot of k_C vs. [Ag(I)] as shown in Fig. 5 [33–35].

Activity of Catalyst

Moelwyn–Hughes [36] observed that both the uncatalyzed and catalyzed reactions proceed together, so that,

$$k_t = k_U + P_C\,[\mathrm{Ag(I)}]^x$$

where k_t is the experimental pseudo–first-order rate constant in the presence of the Ag(I) catalyst, k_U is the pseudo–first order rate constant in the absence of catalyst, P_C is the catalytic constant, and x is the order of the reaction with reference to Ag(I). In the current analysis, x values for the standard reaction run are measured as unity. Then, the value of P_C is determined by the equation given below. The average value of P_C for the reaction was 212 ± 5.0.

$$P_C = \frac{[k_t - k_u]}{[\mathrm{Ag(I)}]^x} = \frac{k_C}{[\mathrm{Ag(I)}]^{1.12}}$$

where $k_t - k_u = k_C$.

The above figure indicates that the rate constant k'_{obs} relies upon on the concentration of catalyst, and it increases with an increase in [Ag^+]. When a graph is plotted for the [Ag^+] concentration vs. the rate constant, a straight line is obtained, representing that the rate is linearly related to the Ag(I) concentration (Fig. 5).

Kinetic Modeling

The reaction of LNZ with FAC in the presence of the Ag(I) catalyst is first order with respect to every reactant and it can be elucidated by using a second-order rate equation:

$$\begin{aligned}\frac{\mathrm{d[LNZ]_T}}{\mathrm{d}t} &= -k'_{obs}[\mathrm{LNZ}]_T \\ &= -k''_{app}[\mathrm{FAC}]_T[\mathrm{LNZ}]_T[\mathrm{Ag^+}]_T \end{aligned} \quad (1)$$

where k'_{obs} is the experimental pseudo–first-order rate constant, T is the total of all acid-base species for a given reactant, and k''_{app}(dm^3 mol^{-1} s^{-1}) is the pH-dependent second-order rate constant for the whole reaction, which can be determined from $k''_{app} = (k'_{obs}/[\mathrm{FAC}]_T[\mathrm{Ag^+}]_T)$. The p$K_a$ of LNZ is 1.8, which means that it is a strong acid; hence LNZ dissociates to form an anion [LNZ^-]. The variation in k''_{app} from pH 4.0 to 9.0 can be ascribed to the changing significance of specific reaction among the individual acid–base speciation of LNZ and FAC in the presence of the Ag(I) catalyst. The results can possibly be understood from Schemes 2 and 3. Similarly, electrophilic halogenation is suggested for enrofloxacin with the FAC reaction and it is relatively well documented with respect to bromination and chlorination reactions [24]. LNZ has a 1,3-oxazolidinone moiety containing an acetamide subgroup at the fifth methyl group position. Owing to the electron-withdrawing inductive effect (−I) of the chlorine atom, the electron-deficient chlorine electrophile susceptible to attacks on the nitrogen atom of the acetamide group leads to formation of a chlorinated product [30]. The major and minor products identified by LC-ESI-MS in the reaction are given in Scheme 1 and Table I.

Rate law: The proposed mechanism of the Ag(I)-catalyzed reaction with LNZ proceeds via an intermediate complex, which decomposed in a slow reaction with FAC, giving rise to a chlorinated product:

$$\mathrm{OCl^-} + \mathrm{H^+} \overset{K_1}{\rightleftharpoons} \mathrm{HOCl} \quad K_1 = 10^{+7.5} \quad (2)$$

$$\begin{aligned}&\mathrm{Complex} + \mathrm{HOCl} \underset{\text{Slow}}{\overset{k}{\rightarrow}} \mathrm{LNZ - Cl} + \mathrm{H_2O} + \mathrm{Co_2} + \mathrm{Ag(I)} \\ &\mathrm{Rate_C} = \mathrm{Rate_T} - \mathrm{Rate_U} \\ &\mathrm{Rate} = k[\mathrm{Complex}] = k[\mathrm{Complex}][\mathrm{HOCl}] \\ &\qquad = kK_2[\mathrm{HOCl}][\mathrm{LFC}][\mathrm{Ag(I)}] \\ &\qquad = kK_1K_2[\mathrm{OCl^-}][\mathrm{H^+}][\mathrm{LNZ}][\mathrm{Ag^+}]\end{aligned} \quad (3)$$

$$\begin{aligned}[\mathrm{LNZ}]_T &= [\mathrm{LNZ}]_f + [\mathrm{Complex}] \\ &= [\mathrm{LNZ}]_f + K_2[\mathrm{LNZ}][\mathrm{Ag^+}]\end{aligned} \quad (4)$$

Hypochlorous acid (HOCl) and hypochlorite (OCl^-) are the main chlorine species, which are called FAC. HOCl is the predominant species below pH 7.5 and OCl^- is predominant above pH 7.5. The decrease in the magnitude of k''_{app} above pH 7.5 can be attributed to deprotonation of HOCl to yield OCl^-, that is generally a much weaker electrophile than HOCl; for this reason HOCl has been considered as the reactive species [32].

$$\begin{aligned}
[\mathrm{LNZ}]_f &= \frac{[\mathrm{LNZ}]_T}{1+K_2[\mathrm{Ag}^+]}\\
[\mathrm{Ag}^+]_f &= \frac{[\mathrm{Ag}^+]_T}{1+K_2[\mathrm{LNZ}]}\\
[\mathrm{OCl}^-]_T &= [\mathrm{OCl}^-]_f + [\mathrm{HOCl}]\\
&= [\mathrm{OCl}^-]_f + K_1[\mathrm{OCl}^-][\mathrm{H}^+] + k[\mathrm{HOCl}][\mathrm{Complex}]\\
&= [\mathrm{OCl}^-]_f + K_1[\mathrm{OCl}^-][\mathrm{H}^+] + kK_1[\mathrm{OCl}^-][\mathrm{H}^+][\mathrm{Complex}]\\
&= [\mathrm{OCl}]_f + K_1[\mathrm{OCl}^-][\mathrm{H}^+] + kK_1K_2[\mathrm{OCl}^-][\mathrm{H}^+][\mathrm{LNZ}][\mathrm{Ag}^+]
\end{aligned} \tag{5}$$

$$[\mathrm{OCl}^-]_f = \frac{[\mathrm{OCl}^-]_T}{1+K_1[\mathrm{H}^+]+kK_1K_2[\mathrm{H}^+][\mathrm{LNZ}][\mathrm{Ag}^+]}$$

$$\begin{aligned}
[\mathrm{OCl}^-]_f &= \frac{[\mathrm{OCl}^-]_T}{1+K_1[\mathrm{H}^+]}\\
[\mathrm{H}^+]_T &= [\mathrm{H}^+]_f + [\mathrm{HOCl}]\\
&= [\mathrm{H}^+]_f + [\mathrm{H}^+][\mathrm{OCl}^-]
\end{aligned} \tag{6}$$

$$[\mathrm{H}^+] = \frac{[\mathrm{H}^+]_T}{1+K_1[\mathrm{OCl}^-]} \tag{7}$$

Substituting the values from Eqs. (4) to (7) in Eq. (3)

$$\mathrm{Rate} = kK_1K_2\left[\frac{[\mathrm{OCl}^-]_T}{1+K_1[\mathrm{H}^+]}\right]\left[\frac{[\mathrm{H}^+]_T}{1+K_1[\mathrm{OCl}^-]}\right] \times \left[\frac{[\mathrm{LNZ}]_T}{1+K_2[\mathrm{Ag}^+]}\right]\left[\frac{[\mathrm{Ag}^+]_T}{1+K_2[\mathrm{LNZ}]}\right]$$

$$\mathrm{Rate} = kK_1K_2 \times \frac{[\mathrm{OCl}^-]_T[\mathrm{H}^+]_T[\mathrm{LNZ}]_T[\mathrm{Ag}^+]_T}{\{1+K_1[\mathrm{H}^+]\}\{1+K_1[\mathrm{OCl}^-]\}\{1+K_2[\mathrm{Ag}^+]\}\{1+K_2[\mathrm{LNZ}]\}} \tag{8}$$

$$\mathrm{Rate} = kK_1K_2\frac{[\mathrm{OC}l^-]_T[\mathrm{H}^+]_T[\mathrm{LNZ}]_T[\mathrm{Ag}^+]_T}{\left\{1+K_1[\mathrm{H}^+]+K_1[\mathrm{OCl}^-]\right\}\left\{1+K_2[\mathrm{Ag}^+]\right\}\{1+K_2[\mathrm{LNZ}]\}}$$

$$\begin{aligned}
\mathrm{Rate} = \frac{kK_1K_2[\mathrm{OCl}^-]_T[\mathrm{H}^+]_T[\mathrm{LNZ}]_T[\mathrm{Ag}^+]_T}{1+K_2[\mathrm{Ag}^+]+K_2[\mathrm{LNZ}]}\\
+K_1[\mathrm{H}^+]+K_1K_2[\mathrm{H}^+][\mathrm{Ag}^+]\\
+K_1K_2[H^+][\mathrm{LNZ}]+K_1[\mathrm{OCl}^-]\\
+K_1K_2[\mathrm{OCl}^-][\mathrm{Ag}^+]\\
+K_1K_2[\mathrm{OCl}^-][\mathrm{LNZ}]
\end{aligned} \tag{9}$$

At very low concentrations of silver and LNZ, Eq. (9) reduces to

$$\frac{\mathrm{Rate}}{[\mathrm{LNZ}]} = k_{obs} = \frac{kK_1K_2[\mathrm{OCl}^-][\mathrm{H}^+][\mathrm{Ag}^+]}{1+K_1[\mathrm{OCl}^-]+K_1[\mathrm{H}^+]} \tag{10}$$

Equation (10) confirms all the observed reaction orders with respect to various species, which can be verified by arranging

$$\frac{1}{k_{obs}} = \frac{1}{kK_1K_2[\mathrm{OCl}^-][\mathrm{H}^+][\mathrm{Ag}^+]} + \frac{1}{kK_2[\mathrm{H}^+][\mathrm{Ag}^+]} + \frac{1}{kK_2[\mathrm{H}^+][\mathrm{OCl}^-]} \tag{11}$$

$$\frac{[\mathrm{Ag}^+]}{k_C} = \frac{1}{kK_1K_2[\mathrm{OCl}^-][\mathrm{H}^+]} + \frac{1}{kK_2[H^+]} + \frac{1}{kK[\mathrm{OCl}^-]} \tag{12}$$

The influence of temperature on the reaction rate in both the catalyzed and uncatalyzed reactions in terms of second-order rate constants is presented in Table IV. From the Arrhenius plot of log k_1 vs. $1/T$, the activation energy was determined, which help us to calculate other activation parameters such as enthalpy of activation, entropy of activation, and Gibbs free energy of activation, and these values are given in Table IV. The results point out that the moderate value of activation energy (E_a) was 14.33 kJ mol^{-1} for the uncatalyzed reaction and for the silver(I)-catalyzed oxidation (E_a) was found to be 12.07 kJ mol^{-1}, which was lower than the uncatalyzed reaction. Entropy of activation $\Delta S^{\#}$ is -257.88 J K^{-1} mol^{-1} for the silver-catalyzed oxidation and for the uncatalyzed reaction it was found to be -12.40 J K^{-1} mol^{-1}. The value of entropy of activation is observed to be negative. The moderately high value of negative $\Delta S^{\#}$ proposes the formation of greatly ordered activated complex with a decrease in the degree of freedom of molecules, with free energy of activation $\Delta G^{\#}$ is 86.95 kJ mol^{-1} for the silver-catalyzed oxidation and 15.54 kJ mol^{-1} for the uncatalyzed reaction. The value of enthalpy of activation ($\Delta H^{\#}$) is 9.58 kJ mol^{-1} for silver-catalyzed oxidation and for uncatalyzed oxidation it was found to be 11.85 kJ mol^{-1}. Metal ions perform as a catalyst by one of these distinct paths, leading to formation of complexes with reactants [37]. An extremely solvated transition state due to the positive value of $\Delta H^{\#}$ and $\Delta G^{\#}$, given in Table IV,

increases the size of transition state; the moderate values of $\Delta H^{\#}$ and $\Delta G^{\#}$ were favorable for electron transfer processes [41,42]. A negative value of $\Delta S^{\#}$ represents that the transition state is more ordered than the reactants [43]. The activation parameters calculated for the catalyzed and uncatalyzed reactions reveal the influence of catalyst on the reaction.

The influence of pH on the kinetics of LNZ with FAC was investigated at different temperatures and different pH. Experiments were done at very acidic, neutral, and very basic conditions. Oxidation rates decrease with increasing pH under reaction conditions. The activation energy values are pH dependent, and we have reported their relative contribution to the overall oxidation rate. The activation energy values reported for both silver(I)catalyzed and uncatalyzed oxidation in Table IV are comparable with the literature.The higher the value of activation energy the faster the acceleration of the oxidation process when temperature increases [44,45].

The Ag(I) catalyst develops a complex (C) with the substrate, which reduces the character of the substrate more than without a catalyst. Therefore, the Ag(I) catalyst alters the reaction by reducing the activation energy. A catalyst functions by providing a different path by lowering the E_a of the reaction. At any given interval of time, the presence of a catalyst allows a greater quantity of the reactant species, gains enough energy to pass through the transition state, and turns reactants into products [20,46].

Monochlorination of LNZ in the presence of Ag(I) catalyst leads to a net mass gain of 34.5 Da relative to the parent LNZ molecule. Similarly, electrophilic halogenation is suggested for the enrofloxacin reaction with FAC and it is comparatively well documented with reference to chlorination reactions [47,49].

It is observed that changing of the ionic strength had insignificant effect on the rate of reaction, which is due to a neutral species or a neutral and a charged species (see Table III) at pH of 5.00, 7.00, and 9 [49]. For a limiting case of a zero angle approach between two dipoles or an ion–dipole system, Amis has shown that a plot log k'_{obs} vs. $1/D$ gives a straight line with a negative slope for reaction between negative ions and dipole. In the present study, the rate constant at pH 7.0 decreases with a decrease in the dielectric constant of the medium. The plot of log k'_{obs} vs. $1/D$ is linear with a negative slope, indicating that the reaction is between a negative ion and a dipole. This supports our mechanism as it involves the reaction between [LNZ^-] and HOCl [50].

CONCLUSION

LNZ readily reacts with FAC at the oxidant concentration and pH environment observed in municipal water chlorination processes. An apparent second-order rate constant for the uncatalyzed reaction, i.e., $k''_{app} = 8.15\ dm^3\ mol^{-1}\ s^{-1}$ at pH 4.00 and $k''_{app.} = 0.076\ dm^3\ mol^{-1}\ s^{-1}$ at pH 9.00 and at 25 ± 0.2°C, and the total evident second-order rate constant for the Ag(I)-catalyzed reaction, i.e., $k''_{app} = 51.50\ dm^3\ mol^{-1}\ s^{-1}$ at pH 4.00 and $k''_{app.} = 1.03\ dm^3\ mol^{-1}\ s^{-1}$ at pH 9.00 and at 25 ± 0.2°C, indicate that LNZ reacts with FAC faster in the presence of catalyst in normal water treatment processes.

The reaction of FAC with LNZ undergoes electrophilic halogenation on the acetamide moiety of LNZ, leading to the formation of a monohalogenated product. Based on the kinetic data and LC/ESI/MS spectra, the mechanism for the LNZ/FAC reaction is proposed, indicating that catalyst does not alter the nature of the product.

The antibacterial activity of LNZ is attributed to oxazolidinone and morpholin moieties. The product of the LNZ/FAC reaction retains both oxazolidinone and morpholin moieties. Hence, the product may preserve the antibacterial activity [16].

BIBLIOGRAPHY

1. Deborde, M.; von Gunten, U. Water Res 2008, 42, 13–51.
2. Kulkarni, R. M.; Malladi, R. S.; Hanagadakar, M. S.; Doddamani, M. R.; Bhat, U. K. Desalin Water Treat 2016, 57, 16111–16118.
3. Kulkarni, R. M.; Hanagadakar, M. S.; Malladi, R. S.; Santhakumari, B.; Nandibewoor, S. T. Prog React Kinet Mech 2016, 41, 245–257.
4. Kayaci, F.; Vem pati, S.; Ozgit-Akgun, C.; Donmez, I.; Biyikli, N.; Uyar, T. Appl Catal B: Environ 2015, 176–177, 646–653.
5. Showkat, A. M.; Zhang, Y. P.; Kim, M. S.; Gopalan, A. I.; Reddy, K. R.; Lee, K. P. Bull Korean Chem Soc 2007, 28, 1985–1992.
6. Reddy, K. R.; Nakata, O. K.; Tsuyoshi; Tryk, T. M.; Donald, F. A. J Nanosci Nanotechnol 2010, 12, 7951–7957.
7. Kulkarni, R. M.; Bhamare V.S.; Santhakumari, B. Desalin Water Treat 2016, 57, 24999–25010.
8. Zhang, Q.; Chen, P.; Zhuo, M.; Wang, F.; Su, Y.; Chen, T.; Yao, K.; Cai, Z.; Lv, W.; Liu, G. Appl Catal, B 2018, 221, 129–139.
9. Kummerer, K. Annu Rev Environ Resour 2010, 35, 57–75.

10. Zhang, H.; Huandang, C. H. Environ Sci Technol 2005, 39(2), 593–601.
11. Alexy, R.; Sommer, A.; Lange, F. T.; Kuemmerer, K. Clean–Soil, Air, Water 2006, 34(6), 587–592.
12. Knapp, C. W.; Cardoza, L. A.; Hawes, J. N.; Wellington, E. M. H.; Larive, C. K.; Graham, D. W. Environ Sci Technol 2005, 39, 9140–9146.
13. Lindstrom, A.; Buerge, I. J.; Poiger, T.; Bergqvist, P. A.; Muller, M. D.; Buser, H. R. Environ Sci Technol 2002, 36, 2322–2329.
14. Parshikov, I. A.; Freeman, J. P.; Lay, J. O.; Beger, R. D.; Williams, A. J.; Sutherland, J. B. Microbiol Lett 1999, 177, 131–135.
15. Wetzstein, H. G.; Stadler, M.; Tichy, H. V.; Dalhoff, A.; Karl, W. Appl Environ Microbiol 1999, 65, 1556–1563.
16. Kulkarni, R. M.; Hanagadakar, M. S.; Malladi, R. S.; Gudaganatti, M. S.; Biswal, H. S.; Nandibewoor, S. T. Ind J Chem Technol 2014, 21, 38–43.
17. Brickner, S. J. Bentham Science Publishers; Schiphol, the Netherlands, 1996; Vol. 2, pp. 175–194, 1381–6128.
18. Wilkinson, S. Chem Eng News 1999, 77, 27–28.
19. Wang, F.; Wang, Y.; Feng, Y.; Yongqin Zeng, Y.; Xie, Z.; Zhang, Q.; Su, Y.; Chen, P.; Liu, Y.; Yao, K.; Lv, W.; Liu, G. Appl. Catal., B 2018, 221, 510–520.
20. Zigang, L.; Chuan, H. Eur J Org Chem 2006, 19, 4313–4322.
21. Cao, E.; Gavriilidis, A. W; Motherwell, B. Chem Eng Sci 2004, 59, 4803–4808.
22. Taquet, J. P.; Siri, O.; Collin, J. P.; Messaoudi, A.; Braunstein, P. New J Chem 2005, 29, 188–192.
23. Mitrano, D. M.; Rimmele, E.; Wichser, A.; Erni, R.; Height, M.; Nowack, B. ACS Nano 2014, 8(7), 7208—7219.
24. Gudaganatti, M. S.; Hanagadakar, M. S.; Kulkarni, R. M.; Malladi, R. S.; Nagarale, R. K. Prog React Kinet Mech 2012, 37, 366–382.
25. Eaton, A. D.; Clesceri, L. S.; Rice, E. W.; Greenberg, A. E. Standard Methods for the Examination of Water and Wastewater, 21st ed.; American Public Health Association: Washington, DC, 2005.
26. American Public Health Association, American Water Works Association, and Water Pollution Control Facility. Standard Methods for the Examination of Water and Wastewater, 20th ed.; American Public Health Association: Washington DC, 1998.
27. Hammerl, A; Klapötke, T. M. In Encyclopedia of Inorganic Chemistry, 2nd ed.; Wiley: Hoboken, NJ, 2005; pp. 55–58.
28. Kulkarni, R. M.; Belihal, D. C.; Nandibewoor, S. T. Inorg React Mech 2002, 3(4), 239–247.
29. Zheng, J. Clinical Pharmacology and Bio Pharmaceitics Review; Washington DC: FDA, 2000; p. 1. Available at https://www.accessdata.fda.gov/drugsatfda_docs/nda/2000/21130_Zyvox_biopharmr.pdf.
30. Richard, D. G. Introduction to Physical Organic Chemistry; Addison Wesley: London, 1970; pp. 195–202.
31. David, R. L. CRC Handbook of Chemistry and Physics, 85 ed., CRC Press: Boca Raton, FL, 2004; pp. 6–15.
32. Kulkarni, R. M.; Hanagadakar, M. S.; Malladi, R. S.; Biswal, H. S.; Cuerda-Correa, E. M. Desalin Water Treat 2016, 57, 10826–10838.
33. Bhattacharya, S.; Benerjee, P. Bull Chem Soc Jpn 1996, 69, 3475–3482.
34. Pol, P. D.; Kathari, C. P.; Nandibewoor, S. T. Trans Met Chem 2002, 27, 807–812.
35. Khan, A. A. A.; Khan, A.; Asiri, A. M.; Khan, S. A. J Mol Liq 2016, 218, 604–610.
36. Moelwyn-Hughes, E. A. Kinetics of Reaction in Solutions; Oxford University Press: London, 1947, p. 297.
37. Morris, C. J. Phys Chem 1966, 70(12), 3798–3805.
38. Kiersikowska, E.; Marai, H.; Wrzeszcz, G.; Kita, E. Trans Met Chem 2013, 38, 603–610.
39. Khan, A. A. P.; Khan, A.; Asiri, A. M.; Azum, N.; Rub, M. A. J Taiwan Inst Chem Eng 2014, 45, 127–133.
40. Khan, A. A. P.; Asiri, A. M.; Azum, N.; Rub, M. A.; Khan, A.; Al-Youbi, A. O. Ind Eng Chem Res 2012, 17, 4819–4824.
41. Pauling, L. The Nature of the Chemical Bond and the Structure of Molecules and Crystals, 3rd ed.; Oxford and IBH: New Delhi, India, 1969; p. 496.
42. Munavalli, D. S.; Naik, P. N.; Ariga, G. G.; Nandibewoor, S. T.; Chimatadar, S. A. Cogent Chem 2015, 1, 510.
43. Wisńiewska, J.; Kita, P.; Wrzeszcz, G. Trans Met Chem 2007, 32, 857–863.
44. Marisa, R.; Javier Huertas, F.; Brady, P. V. Geochim Cosmochim Acta 2009, 73(13), 3752–3766.
45. Quantitative analysis of chemical and biological kinetics for the acid mine drainage problem; Mend project 1.51.1.
46. Dodd, M. C.; Shah, A. D.; von Gunten, U.; Huang, C. H. Environ Sci Technol 2005, 39, 7065–7076.
47. Boyce, S. D.; Hornig, J. F. Environ Sci Technol 1983, 17, 202–211.
48. Itoh, S. I.; Naito, S.; Unemoto, T. Water Res 1985, 19, 1305–1309.
49. Laidler, K. J. Chemical Kinetics, 3rd ed.; Pearson Education: New Delhi, India, 2004; p. 183.
50. Amis, E. S. Chemical Kinetics: Solvents Effects on the Rate of Mechanisms; Academic Press: New York, 1966.